JOURNAL OF GEOPHYSICAL RESEARCH, VOL. 111, C09021, doi:10.1029/2005JC002963, 2006

Hydrography of the southern Bay of Biscay shelf-break region: Integrating the multiscale physical variability over the period 1993–2003

Marcos Llope,[1,2] Ricardo Anadón,[1] Leticia Viesca,[1] Mario Quevedo,[1]
Rafael González-Quirós,[1,3] and Nils C. Stenseth[4,5]

Received 18 March 2005; revised 4 May 2006; accepted 23 May 2006; published 15 September 2006.

[1] The southern Bay of Biscay (NW Spain) shows a very active hydrography due to the different origins of its Central Waters, the local modifications exerted on them by continental effects and the recurrence of mesoscale processes such as slope currents, upwellings and eddies. In order to assess the role of the different sources of variability we conducted a monthly series of CTD sampling in the central Cantabrian Sea along a coastal-oceanic transect, from 1993 to 2003. We analyzed the spatial variability of the hydrographic processes over different timescales. The thermohaline properties of Central Waters varied between those typical of the subpolar mode of the Eastern North Atlantic Central Water (ENACWsp) and a local mode, the Bay of Biscay Central Water (BBCW), though there has been a clear shift toward the BBCW prevalence in the last years. The Iberian Poleward Current (IPC) conveyed subtropical Central Waters (ENACWst) into the region almost every winter. This slope current may display a double-core structure during some extreme events. The upper layers of the ocean showed a long-term trend toward increasing temperature and decreasing salinity, and accordingly density was on the decrease. These patterns suggest an enhancement of the water column stratification. Coastal upwellings are an important source of inshore variability and counteract these long-term changes on the coast. However, their intensity seems to be decreasing and their seasonal pattern changing toward a general advancement of the upwelling-favorable season.

Citation: Llope, M., R. Anadón, L. Viesca, M. Quevedo, R. González-Quirós, and N. C. Stenseth (2006), Hydrography of the southern Bay of Biscay shelf-break region: Integrating the multiscale physical variability over the period 1993–2003, *J. Geophys. Res.*, *111*, C09021, doi:10.1029/2005JC002963.

1. Introduction

[2] Ocean margins are very rich ecosystems in terms of hydrographic diversity as they integrate the oceanic, atmospheric and continental forcing [*Mann and Lazier*, 1991; *Holligan and Reiners*, 1992]. This high hydrographic variability ultimately controls the structure of the coastal food webs [*Kiørboe*, 1993; *Falkowski et al.*, 1998]. Thus any change in the strength or timing of the involved hydrographic processes could have major consequences on the biological productivity including marine renewal resources, for example, fisheries [*Beaugrand et al.*, 2003].

[3] Much interest has recently been devoted to understanding the responses of marine systems to global change (see GLOBEC project, www.globec.org). A critical challenge is the separation of anthropogenic forcing from natural variability. To reliably detect any eventual signal of change in the dynamic coastal system, it is necessary to disentangle the different sources of hydrographic and atmospheric forcing, as well as to characterize their range of variability. Oceanographic monitoring programs, based on regular records of water column profiles, proved to be particularly valuable, for example, the Hawaii (HOT) and Bermuda (BATS) research programs [*Karl and Michaels*, 1996; *Siegel et al.*, 2001]. These series have provided important background information regarding past variation as well as a quantification of the intrinsic noise associated to each hydrographic process. Data from such programs allow us, unlike what is the case with satellite-based telemetry, to look beneath the surface, and they grant an integrated view of different-scale processes.

[4] In the present study we aim at better resolving the spatial and temporal scales of hydrographic processes in the southern Bay of Biscay. To do so, we conducted a monthly

[1] Área de Ecología, Departamento de Biología de Organismos y Sistemas, Universidad de Oviedo, Oviedo, Spain.
[2] Now at Centre for Ecological and Evolutionary Synthesis (CEES), Department of Biology, University of Oslo, Oslo, Norway.
[3] Now at Centro de Investigación y Formación Acuícola y Pesquera El Toruño, Cádiz, Spain.
[4] Centre for Ecological and Evolutionary Synthesis (CEES), Department of Biology, University of Oslo, Oslo, Norway.
[5] Also at Flødevigen Marine Research Station, Institute of Marine Research, His, Norway.

0148-0227/06/2005JC002963

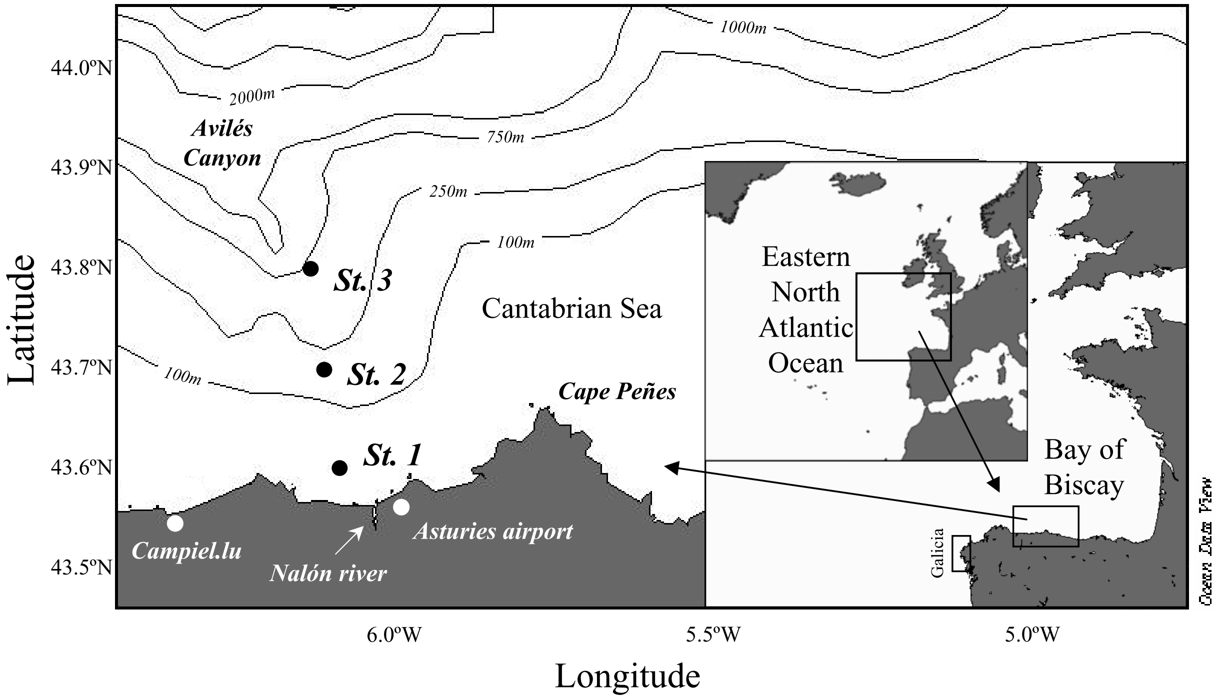

Figure 1. Sampling area, the Cantabrian Sea (South Bay of Biscay) showing the position of the three stations: Station 1, Station 2, Station 3 (black dots), the meteorological station at Asturies airport, and the location of the continuous thermometer at Campiel.lu (white dots).

time series of CTD profiles from 1993 to 2003 consisting of three stations along a coastal-oceanic transect.

[5] The Bay of Biscay is a Large Marine Ecosystem [*Sherman and Skjoldal*, 2002]. It is located in an intergyre zone enclosed by the subpolar and subtropical gyres [*Pollard et al.*, 1996]. As a result, two subtypes of Central Waters (Eastern North Atlantic Central Water, ENACW) have been defined: the subpolar (ENACWsp) and subtropical (ENACWst) modes [*Pérez et al.*, 2001]. A third water body formed by diapycnal mixing on the Armorican-Celtic shelf [*Cooper*, 1949] has also been described: the Bay of Biscay Central Water (BBCW) [*Fraga et al.*, 1982; *Botas et al.*, 1989], first called Gulf Water (G) by *Tréguer et al.* [1979]. However, other authors consider that its thermohaline imprint falls within the range of variation of the ENACW and avoid the use of this name.

[6] The Iberian Poleward Current (IPC) conveys subtropical waters into the bay [*Frouin et al.*, 1990; *Haynes and Barton*, 1990; *Ambar and Fiúza*, 1994]. This slope current, also referred to as Portugal Coastal Counter Current (PCCC) [*Álvarez-Salgado et al.*, 2003] or Navidad [*Pingree and Le Cann*, 1992a, 1992b], circulates poleward along the Portuguese coast, to turn eastward and run along the Cantabrian continental shelf and slope and, eventually, reach the Armorican shelf off SW France at 47°N [*Pingree and Le Cann*, 1990; *García-Soto et al.*, 2002]. The IPC appears mostly in winter [*Botas et al.*, 1988; *Gil*, 2003] associated to the upwelling/downwelling regime off the western Iberian Peninsula [*Álvarez-Salgado et al.*, 2003]. Its physical, chemical [*Álvarez-Salgado et al.*, 2003, and references therein], and biological implications [*Fernández et al.*, 1993; *Bode et al.*, 2002; *Huskin et al.*, 2003; *Isla and Anadón*, 2004] have been well studied. However, there is little information about the year-to-year recurrence, intensity, temporal trends and vertical structure of this phenomenon based on time series detection, except for sea surface temperature (SST) satellite images [*Frouin et al.*, 1990; *Pingree and Le Cann*, 1990; *García-Soto et al.*, 2002].

[7] Wind-driven upwelling [*Molina*, 1972; *Botas et al.*, 1990; *Gil et al.*, 2002] is another important process. During summer, it brings nutrients into the depleted upper layers of the ocean and therefore directly affects coastal primary production and food web structure.

[8] There is also the strong seasonal cycle of stratification/mixing that typically drives ocean dynamics at these latitudes. The occurrence of all these hydrographic processes in the Cantabrian Sea makes it a suitable place to study their forcing on the bay, and permits a multilayered analysis: (1) the large-scale interannual variation of Central Waters; (2) the mesoscale processes: slope currents and upwellings in relation to the atmospheric forcing; and (3) the combined effect of all these processes on the seasonal and long-term variability of temperature and salinity at different depths in the water column as well as the implications they have on seasonal stratification.

2. Data and Methods

2.1. Study Area and Sampling Scheme

[9] The Cantabrian Sea is the southernmost part of the Bay of Biscay, in the eastern North Atlantic (Figure 1). The presence of Cape Peñes is known to reinforce wind-driven upwellings to the west [*Blanton et al.*, 1984; *Botas et al.*, 1988].

[10] Three permanent stations situated along a transect perpendicular to the coast (Figure 1) were sampled on a

Table 1. Temperature Long-Term Trends[a]

	Station 3				Station 2				Station 1			
		Slope				Slope				Slope		
	Seas, %	Percent	°C yr^{-1}	P Value	Seas, %	Percent	°C yr^{-1}	P Value	Seas, %	Percent	°C yr^{-1}	P Value
10 m	***90.8***	***0.51***	*0.055*	*0.025*	***89.2***	***0.36***	*0.043*	*0.067*	**82.3**	-	0.021	0.409
20 m	***87.4***	***0.72***	*0.056*	*0.027*	**77.9**	-	0.023	0.408	**74.5**	-	0.010	0.710
30 m	**73.1**	-	0.031	0.275	**62.4**	-	0.015	0.604	**67.6**	-	0.000	0.989
40 m	**64.5**	-	−0.004	0.886	**49.5**	-	−0.015	0.581	**57.0**	-	0.000	0.991
50 m	**57.0**	-	−0.002	0.941	**43.6**	-	−0.022	0.383	**48.8**	-	−0.012	0.668

[a]Seasonality was highly significant in all cases (p values < 0.001, not shown). The fraction of total variance accounted by the seasonal cycle (r^2) is shown in bold. Slope and significance (p value) of the long-term trend is shown for all depths and stations (either significant or not). Significant trends (p value < 0.1) are italicized, and the percentage of variance is shown for them (boldface). Dashes denote negligible amounts.

monthly basis from December 1992 to December 2003. Coastal Station 1 (St. 1; 43°36′N, 06°08′W, maximum depth 65 m) is 7 km offshore and was sampled down to 50 m, Station 2 (St. 2; 43°42′N; 06°09′W, max. depth 135 m) is a shelf station (16.7 km) sampled down to 100 m, Station 3 (St. 3; 43°46′N, 06°10′W, max. depth 870 m) on the slope (23.4 km) is the most oceanic station sampled down to 500 m. These stations are within the long-term monitoring program of the Instituto Español de Oceanografía (IEO, www.seriestemporales-ieo.net).

[11] From December 1992 to April 1993 the sampling was carried out by deploying Niskin oceanographic bottles at discrete depths. Temperature was measured using Watanabe reversible thermometers attached to the bottles whereas salinity was determined by means of Watanabe MKIII induction salinometer calibrated with normal water (I.A.P.S.O.). Salinity in practical salinity units (psu) and density (sigma-*t*, Kg m^{-3}) was calculated as specified in *U. N. Educational, Scientific and Cultural Organization* [1984]. From May 1993 onward, vertical profiles of temperature, salinity and pressure were collected by means of a SBE 25 CTD. The CTD probe was regularly calibrated by the Marine Technology Unit team (www.utm.csic.es) until 2002. From 2002 onward, we have been using a rosette/CTD belonging to the IEO after intercalibration with the previous CTD series. Casts were averaged by 2 meters and salinity (S), density and potential temperature (Θ, deg C) was derived from them; the latter is used throughout the study and will hereafter be referred to as temperature. The outermost station (St. 3) lacked data for 23.3% of the months due to rough sea conditions, this percentage was of 14.3 and 15.8% at St 2 and St. 1, respectively. Most of the missing sampling dates belong to the years 1996–1997.

2.2. Temperature-Salinity

[12] Temperature-salinity diagrams (Θ-S) are used to illustrate the conservative properties of Central Waters. The ENACW and BBCW modes have been previously characterized in the area by *Botas et al.* [1989] and their reference lines are included in the plots: the ENACW ranging from 11°–13°C and 35.53–35.74 and the BBCW from 11°–11.8°C and 35.53–35.58. The limit between the subtropical and subpolar modes of the ENACW was established at 12.20°C and 35.66 by *Ríos et al.* [1992] from cruises carried out during the 1980s. However, it is possible that this limit may have changed after the salinity increase of the 1990s [see *Pérez et al.*, 1995, 2000]. The temporal evolution of salinity was followed at the main core of the Central Waters, on the isopycnal level of 27.1 [*Pérez et al.*, 2001; *González-Pola et al.*, 2005]. Apart from our data set, we also used CTD data of four stations off Galicia (NW Spain) from the cruise GIGOVI-II.

2.3. Time Series Selection and Data Management

[13] Temperature, salinity and density series were studied at different depths depending on the processes we wanted to characterize. Ten meters depth was chosen to show the seasonality of surface temperature because at this depth, the warming and cooling of upper layers is efficiently resolved while the rapid heat exchanges occurring at the atmosphere-ocean interface are attenuated. At 50 m we studied the modification of this cycle below the seasonal thermocline.

Table 2. Salinity Long-Term Trends[a]

	Station 3				Station 2				Station 1			
		Slope				Slope				Slope		
	Seas, %	Percent	yr^{-1}	P Value	Seas, %	Percent	yr^{-1}	P Value	Seas, %	Percent	yr^{-1}	P Value
10 m	-	***5.10***	*−0.015*	*0.024*	-	**1.25**	−0.007	0.238	-	-	−0.002	0.729
20 m	-	***8.16***	*−0.017*	*0.004*	-	***4.07***	*−0.010*	*0.032*	-	-	−0.009	0.100
30 m	-	***8.11***	*−0.014*	*0.004*	-	***9.48***	*−0.012*	*0.001*	-	***3.59***	*−0.010*	*0.047*
40 m	-	***11.7***	*−0.013*	*0.000*	-	***11.0***	*−0.011*	*0.000*	-	***5.00***	*−0.011*	*0.018*
50 m	-	***14.6***	*−0.013*	*0.000*	-	***12.0***	*−0.011*	*0.000*	-	***5.55***	*−0.010*	*0.022*
75 m	-	***15.1***	*−0.010*	*0.000*	-	***13.7***	*−0.010*	*0.000*				
100 m	-	***18.8***	*−0.010*	*0.000*	-	***7.93***	*−0.007*	*0.010*				
200 m	***42.4***	*10.2*	*−0.005*	*0.000*								
300 m	***39.9***	*7.27*	*−0.004*	*0.004*								

[a]Slope, significance (p value) and fraction of total variance (r^2) at 10, 20, 30, 40, 50, 75, 100, 200, and 300 m. The italicized entries correspond to those depths at which salinity trends are significant. The fraction of variance explained by the seasonal cycle (r^2) is shown in bold when significant (p values <0.001 not shown) and separated from the trend. Dashes denote negligible amounts.

Table 3. Density Long-Term Trends[a]

	Station 3				Station 2				Station 1			
		Slope				Slope				Slope		
	Seas, %	Percent	kg m^{-3} yr^{-1}	P Value	Seas, %	Percent	kg m^{-3} yr^{-1}	P Value	Seas, %	Percent	kg m^{-3} yr^{-1}	P Value
10 m	***84.2***	***1.29***	*−0.022*	*0.006*	***80.7***	***0.59***	*−0.013*	*0.076*	**68.2**	-	−0.006	0.478
20 m	***81.0***	***2.18***	*−0.024*	*0.002*	**66.2**	-	−0.010	0.254	**60.9**	-	−0.008	0.308
30 m	***57.7***	***1.35***	*−0.014*	*0.098*	**49.9**	-	−0.010	0.199	**53.8**	-	−0.006	0.432
40 m	**49.9**	-	−0.006	0.408	**38.6**	-	−0.003	0.668	**45.2**	-	−0.007	0.341
50 m	**45.5**	-	−0.006	0.303	**36.3**	-	−0.002	0.758	**40.5**	-	−0.004	0.564

[a]Seasonality was highly significant in all cases (p values < 0.001, not shown). The fraction of total variance accounted by the seasonal cycle (r^2) is shown in bold. Slope and significance (p value) of the long-term trend is shown for all depths and stations (either significant or not). Significant trends (p value < 0.1) are italicized, and the percentage of variance is shown for them (bold type). Dashes denote negligible amounts.

We looked for the seasonal imprint of the IPC on temperature and salinity at 200 and 300 m. Long-term processes such as warming, freshening and their combined implications in stratification were analyzed with much higher resolution, every 10 m (see Tables 1, 2 and 3). As the statistics, based on multiple regression (see statistical tools), did not require the interpolation of missing values, all results are derived from raw data.

2.4. Ekman Transport

[14] The component of the Ekman transport along the y axis (i.e., offshore-inshore owing to the coastline orientation) was estimated according to equation (1) first described by *Bakun* [1973] and later adapted for the Iberian Peninsula by *Lavín et al.* [1991],

$$Q_y = \frac{\tau_x}{f.\rho_w} = \frac{\rho_a.C_d.v_x.|v|}{f.\rho_w}, \qquad (1)$$

where τ_x represents the wind stress along the x axis being ρ_a the density of the air considered constant at 1.22 kg m^{-3}, C_d is an empirical dimensionless drag coefficient considered constant at 0.0014 according to *Hidy* [1972], v_x is the east-west component of the wind, the one inducing upwelling due to the local shoreline orientation, and $|v|$ is the module of the wind, $f = 2\Omega \sin \Phi$ is the Coriolis parameter, approximately 9.96 10^{-5} s^{-1} (43°N) at the time series latitude and ρ_w is the seawater density (1025 kg m^{-3}). Positive values of the Ekman transport mean masses of water (in m^3 s^{-1} km^{-1}) displaced off the coast; this loss is considered to be replaced by deeper, cooler and nutrient-enriched water, i.e., upwelling [*Wooster et al.*, 1976], unlike negative values which produce the opposed phenomenon (i.e., downwelling).

[15] The index was calculated using local wind records. The Instituto Nacional de Meteorología supplied wind strength and direction from the nearby Asturies airport meteorological station (43°33′N, 06°01′W, 127 m asl) (Figure 1). Wind intensity values lower than 6 km h^{-1} were not available for the whole time series so they were removed to make it fully comparable. Three upwelling index values were subsequently calculated per day from wind records taken at 7:00, 13:00 and 18:00 h and then averaged to obtain both daily (n = 12936) and monthly indices (n = 425) from 1968 to 2003.

[16] To show the representativeness of the index, we made use of a high-frequency temperature series recorded with a continuous data logger (ONSET Computer Corporation) at Campiel.lu (43°33′N, 06°24′W) (see Figure 1). Daily temperatures corresponding to high tide were extracted from the series.

[17] To assess the quantitative validity of the index, we compared them with another index computed in the same way but using data winds taken by the buoy Rayo (www.puertos.es), very close to St. 3 and at sea level. The daily regression line was Y = 5.4X − 57.7; r^2 = 0.84. As the fit was quite good we used the airport series because of its much longer temporal resolution. However, the range of upwelling/downwelling values may be underestimated compared to those at sea level.

2.5. North Atlantic Oscillation (NAO) and Local Meteorological Variables

[18] The NAO index is the difference between the normalized sea level pressure between Stykkisholmur (Iceland) to represent the Iceland Low and Ponta Delgada (Azores) to represent the Azores High [*Stenseth et al.*, 2003; *Hurrell*, 1995]. Here we used the monthly data provided by the Climate Prediction Center (NOAA) (ftp://ftpprd.ncep.noaa.gov/pub/cpc/wd52dg/data/indices/tele_index.nh).

[19] The Instituto Nacional de Meteorología supplied series of evaporation, precipitation, relative humidity and air temperature from the airport meteorological station. Series of river runoff for the Nalón River (Figure 1) were supplied by the Confederación Hidrográfica del Norte.

2.6. Statistical Tools

[20] The time series described above can be seen as consisting of three key different components, which can be studied independently since they have different statistical and ecological meanings [*Legendre and Legendre*, 1998]. Typically, there is a seasonal component, a long-term trend component and a random or noise component [*Chatfield*, 1992]. To characterize them, we carried out dummy-variable seasonal regression as this approach enables additive seasonal adjustment to be performed as part of the trend regression model and tolerates missing values. The trend was assumed to be linear and entered into the regression model as a sequential number (expressing time position from

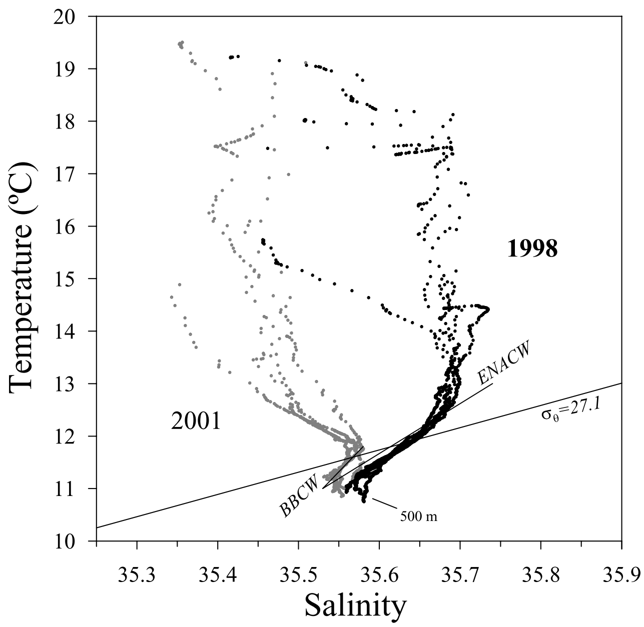

Figure 2. Potential temperature-salinity diagram showing the two subtypes of Central Waters: ENACW in 1998 (black dots) and BBCW in 2001 (gray dots). The reference lines for BBCW and ENACW (see section 2) and the 27.1 isopycnal are shown.

the first observation). The seasonal frame was built as a set of indicator (or dummy) variables and entered as independent regressors. These variables assume the values of either 0 or 1; that is, the indicator for Jan takes a value of 1 in January and 0 for the rest of the year. We used 11 monthly indicators for 11 of the 12 months. The twelfth month is reserved as a baseline for comparison and computed afterward [*Draper and Smith*, 1981]. Being ε_t the stochastic component, we may write the whole model as

$$Y_t = a + bt + c_1 Jan_t + c_2 Feb_t + \ldots + c_{11} Nov_t + \varepsilon_t, \quad (2)$$

where a is the intercept and b is the slope of the trend while each of the c coefficients determines the effect of the month on the level of the series, i.e., the seasonal cycle. Once the series were fitted, we tested the assumptions of linear regression (linearity, independence, homoscedasticity and normality) in the residuals to check the accurateness of the coefficients. Other time series procedures such as Seasonal Decomposition (Census I) or Exponential Smoothing [*Makridakis et al.*, 1983; *Makridakis and Wheelwright*, 1989; *Montgomery et al.*, 1990], not based on regression, were also tested and provided similar values.

3. Results

3.1. Water Masses

[21] Central Waters extend from a subsurface salinity maximum at 50–100 m to a salinity minimum at around 450–500 m, beyond this depth they start mixing with the intermediate Mediterranean Sea Outflow Water (MSW) [*van Aken*, 2000]. The most oceanic station (St. 3), sampled down to 500 m (see map, Figure 1), allowed us to describe the interannual variability. There were periods during which the thermohaline properties were typical of the ENACWsp, like 1998, while others were clearly of the BBCW, like 2001 (Figure 2). The recurrence and prevalence of each form can be tracked through the evolution of salinity at its core, on the 27.1 isopycnal (Figure 3). The highest salinity values, which would correspond to the ENACWsp, appeared around 1993–1994 and 1998–1999 separated by two periods of low salinity (indicating BBCW); the first one was centered around 1995 while the second one stretched from 2001 toward the end of the record.

[22] Local series of evaporation, rainfall, P-E and river runoff were studied with regard to this variation, but no relation was found (not shown). However, the accumulated monthly anomalies of the NAO index showed a pattern opposed to that of salinity. There were two periods of increasing NAO which were followed by decreasing salinity (1993–1995 and 2000–mid-2001), a central period of decreasing NAO and increasing salinity (1996–1999) and a period of little variation at the end of the series (from mid-2001 onward). The whole data set showed no significant relation, probably owing to this last period. The inclusion of more values (to June 2005) made the series significantly correlate in two periods (before and after 1998). The presence of isolated peaks of salinity reflects the sudden intrusions of the ENACW subtropical mode, advected by the IPC.

3.2. The Iberian Poleward Current (IPC)

[23] In November 1999, *Isla and Anadón* [2004] reported the onset of an IPC off Galicia (Figure 4a). This event was also captured by our time series 5 days later (9 November). In Figure 4b, we compare our records with those from Galicia before and during the IPC flow. Its thermohaline imprint was clearly distinguishable from the previous conditions at both places.

[24] By using the same T-S approach we tracked its temporal and vertical evolution during two different winters: 1998–1999 and 2001–2002 (Figure 5), corresponding to ENACWsp and BBCW. In December 1998 (Figure 5a), the IPC showed an incipient development stage with a maximum of salinity at 86 m. In January, when it was fully developed it

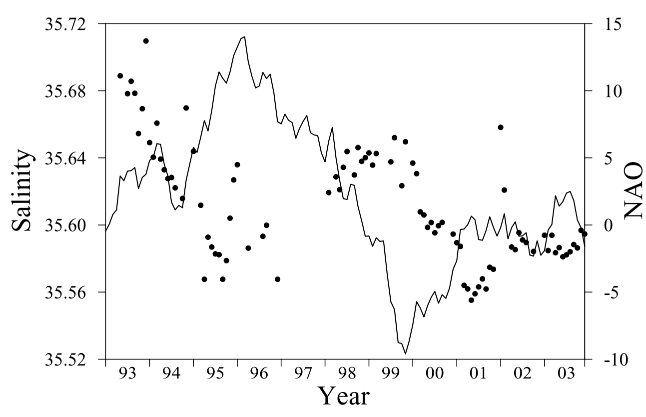

Figure 3. Interannual variation of salinity on the 27.1 isopycnal at Station 3 and the accumulated monthly anomalies of the NAO index. The NAO series is moved forward 1 year. The isolated peaks of salinity spread all through the series reveal the IPC intrusions. Note that the 1997–1998 period is missampled.

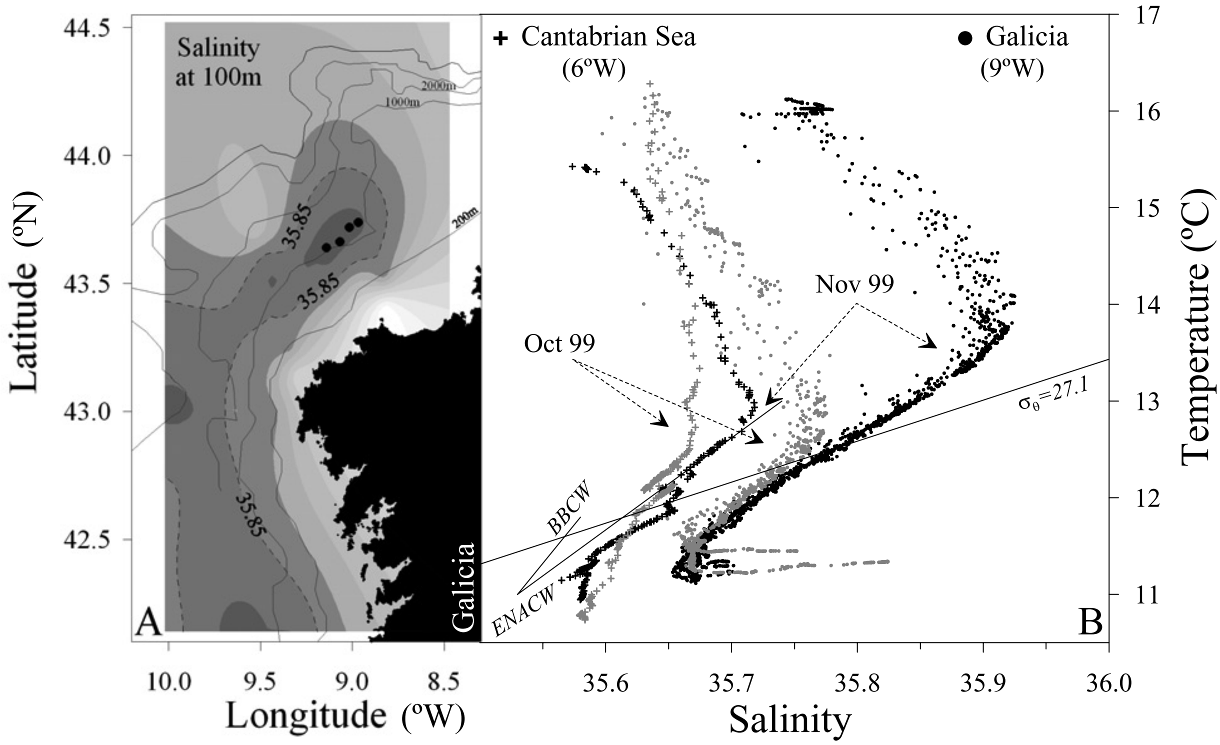

Figure 4. (a) Salinity isolines (spacing 0.05) at 100 m depth off the west coast of Galicia (see Figure 1) in November 1999. The dashed line (salinity > 35.85) corresponds to the core of the IPC (modified from *Isla and Anadón* [2004]). The four dots are the GIGOVI-II stations shown in Figure 4b. (b) Temperature-salinity diagrams at St. 3 (crosses) and Galicia (points). October values (no IPC) are represented by gray symbols, and November 1999 (IPC flow) are represented by black symbols.

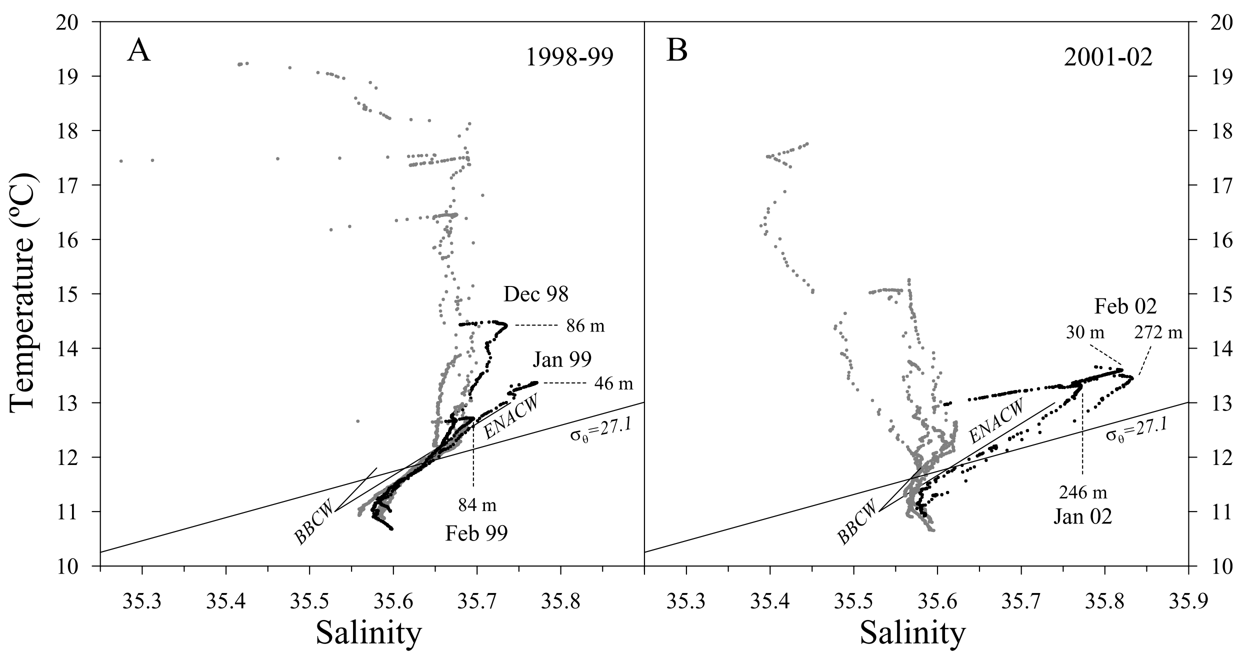

Figure 5. Temperature-salinity diagrams centered on the winters of (a) 1998–1999 and (b) 2001–2002 at Station 3. The reference lines for BBCW and ENACW (see section 2) and the 27.1 isopycnal are shown. Those months showing thermohaline properties of the IPC (ENACWst) are shown in black and the depth of the maximum of salinity, i.e., the IPC core, is indicated.

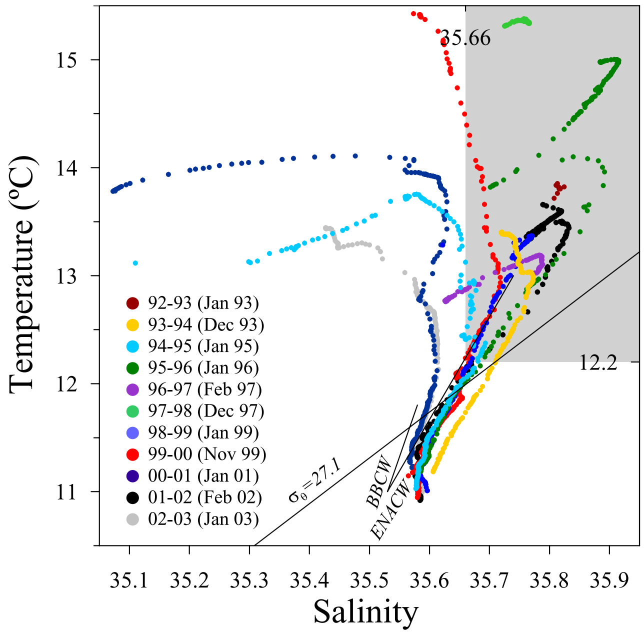

Figure 6. Temperature-salinity diagrams of the most prominent IPC events documented each winter (November–February) from 1992–1993 to 2002–2003 at Station 3 (500 m). The shadowed box delimits the subtropical mode of the ENACW, i.e., the IPC events (see section 2). For those winters showing no IPC structure, January was plotted. Note that 1993 was sampled using Niskin bottles and so it is a discrete profile. February 1997 was sampled down to 200 m but detected the IPC core. Owing to lack of data at St. 3 in 1997–1998, St. 2 is shown instead (100 m); it is therefore highly likely that the IPC event that year was even stronger, as its core seems to have been deeper than 100 m.

was also most shallow (46 m) to sink next month to 84 m. The presence of the BBCW in the winter of 2001–2002 made the current extremely evident, apart from its high intensity (Figure 5b). Interestingly, in February when it was most intense, it showed a singular structure of two salinity cores at 30 and 272 m with no density instabilities.

[25] The presence of IPC, as followed by T/S diagrams, was recorded every winter except for 2000–2001 and 2002–2003. Despite being a typical winter phenomenon (November–February), it may also appear in other seasons [*Fernández et al.*, 1991, 1993; *González-Quirós et al.*, 2004], although less frequently. We investigated the interannual variability by comparing the most intense events recorded each winter (Figure 6). The winters of 1992–1993, 1993–1994, 1995–1996, 1996–1997, 1997–1998, 1998–1999 and 2001–2002 showed marked IPC episodes while there was a weak signal in 1994–1995 and 1999–2000. In contrast, January 2001 and 2003 showed no clear IPC structure and the same happened during the preceding and following months.

[26] As can be seen, temperatures at the surface (SST) showed great variability. January 2001 was one of the warmest, reaching 13.78°C at 2 m, but showed the lowest salinity values of the series. In contrast, the marked IPC episode of 2002 reached a relatively low temperature of 12.97°C.

[27] Regarding its vertical structure, another double-core event was observed in January 1996, with two peaks at 36 and 267 m. Apart from the latter and February 2002, the rest of series showed only one major core at very variable depths depending on the year (Figure 7a). Concerning the atmospheric forcing, the IPC showed no clear response to the winter NAO index of the previous year (Figure 7b) as strong IPCs developed under both positive and negative NAO indices. The averaged November–February downwelling index did not correlate with the strength either (Figure 7c). Moreover, most of the highest salinity values coincided with weak downwelling conditions. We also checked the effect of the upwelling index off Galicia (43°N,11°W from *Lavín et al.* [2000]), since wind direction at the source of the IPC could affect the strength of its flow in the region, but no clear relation was found (not shown).

3.3. Upwelling

[28] Winds affect hydrography on a much shorter temporal scale. This wind-driven upwelling system consists of short-lived upwellings that are efficiently captured by continuous temperature records (Figure 8). Our CTD sampling frequency is too coarse to study them but we can do it in the wind series.

[29] The daily upwelling/downwelling index (1968–2003) may, as a whole, be regarded as a very noisy series made of short positive and negative periods (Figure 9a). Neither the daily nor the average monthly series showed any long-term trend. Despite its high variability, the monthly series showed a significant seasonal component accounting for the 24.1% of total variability. This underlying seasonality resembles much the alternating wind regime of the NW coast of Iberia (i.e., upwelling versus downwelling seasons [see *Álvarez-Salgado et al.*, 2003]). However, instead of presenting a clear positive season, the index hardly exceeds the 0 level in the central months of the year (Figure 9b).

[30] To focus on the recurrence of the positive periods, we studied variations in the number of days with upwelling and intensity of theses days. First, we studied the period from March to September: The intensity showed a negative trend (slope = -2.06 m^3 km^{-1} s^{-1} yr^{-1}, $p = 0.013$) while the number of days slightly increased (0.41 d yr^{-1}, $p = 0.048$). Regarding its seasonality, the number of days showed a dome-shape pattern with a maximum in July. The intensity was higher in March and April than the rest of months which followed a similar pattern to days (Figure 10a). These smoothed cycles showed decadal variations: During the 1990s, the intensity was lower than the previous decades (Figure 10b) but the cycle structure did not vary much. The number of days showed greater decadal variation (Figure 10c), from the dome shape in the 1970s to a more irregular pattern in the 1990s, with a striking maximum in March.

[31] The upwelling season is traditionally considered to extend from April to September [*Bakun*, 1990, *Lavín et al.*, 2000; *Álvarez-Salgado et al.*, 2003]. To make our results comparable with previous studies, we reanalyzed the series excluding March (see Figure 10d). The intensity kept the decreasing trend (slope = -1.75 m^3 km^{-1} s^{-1} yr^{-1}, $p = 0.021$) but there was no change in the number of days ($p = 0.255$).

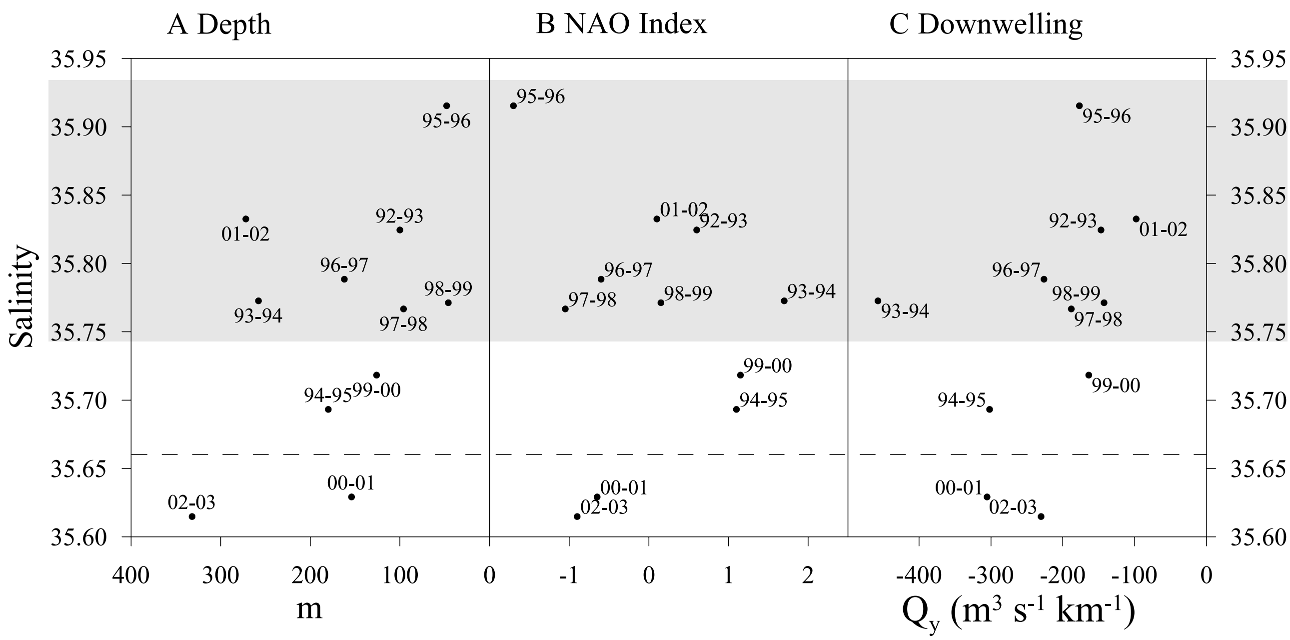

Figure 7. Relation between the maximum value of salinity recorded in the water column each winter at Station 3 (see Figure 5) and (a) the depth at which it appeared, (b) the November–December NAO index, and (c) the downwelling index for the November–January period. The shadowed area contains the strongest IPCs. The horizontal line at 36.66 (see section 2) shows the limit between the ENACWst and ENACWsp, i.e., IPC/no-IPC. Note that owing to lack of information on 1997–1998 at St. 3, St. 2 is shown instead and that this value may be misrepresenting the salinity maximum that winter as St. 2 is only sampled down to 100 m.

3.4. Time Series of Temperature

[32] Figure 11 shows the seasonal cycle along the coastal-oceanic transect at 10 and 50 m. At the surface, positive deviations of temperature stretched typically from June to November (July Nov at St. 1). On the continental shelf and slope (St. 2 and St. 3), the warmest month proved to be August while on the coast (St. 1) the highest temperatures appeared in September. At 50 m, positive deviations extended from September to December. This period is 2 months lagged with regard to the surface and represents the downward transfer of heat due to mixing but also the effect of summer upwelling.

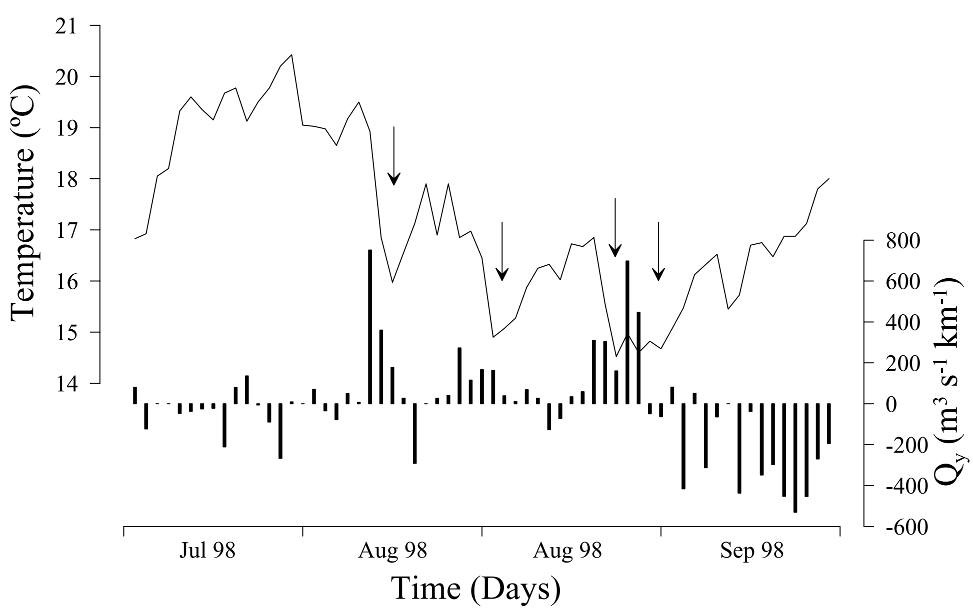

Figure 8. Daily surface temperature (line, see section 2) at Campiel.lu (see map in Figure 1) and the corresponding Ekman transport (bars) at Asturies airport. The arrows indicate sharp decreases of temperature after a few days of upwelling (positive values, offshore transport).

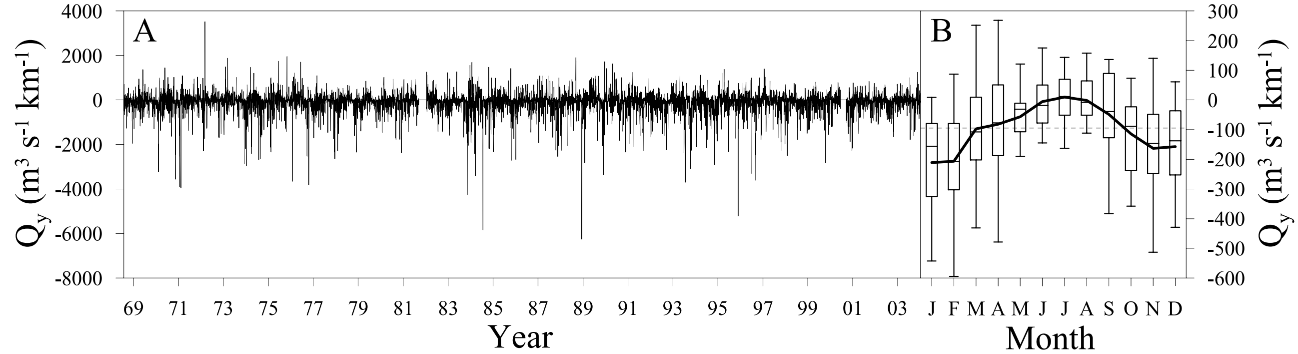

Figure 9. (a) Ekman transport index series calculated from daily wind records at Asturies airport meteorological station (1968–2003). Positive (negative) values indicate upwelling (downwelling) conditions. (b) Box-whisker plot showing the seasonal distribution of the monthly upwelling index. The monthly mean (straight line) and the annual mean of the series (dashed line) are overlaid.

[33] Significant trends of more than 0.05°C yr^{-1} were detected at 10 and 20 m at the outermost station while the middle station (St. 2) presented a marginally significant trend of 0.04 °C yr^{-1} (p value = 0.067) at 10 m (Table 1). The most coastal station (St. 1) showed no significant positive trends. A strong seasonal signal was detected at every depth, being most important at the surface of the outermost station.

3.5. Time Series of Salinity

[34] Salinity did not show a recognizable seasonal cycle above 200 m (Table 2) but it did at 200 and 300 m (Figure 12).

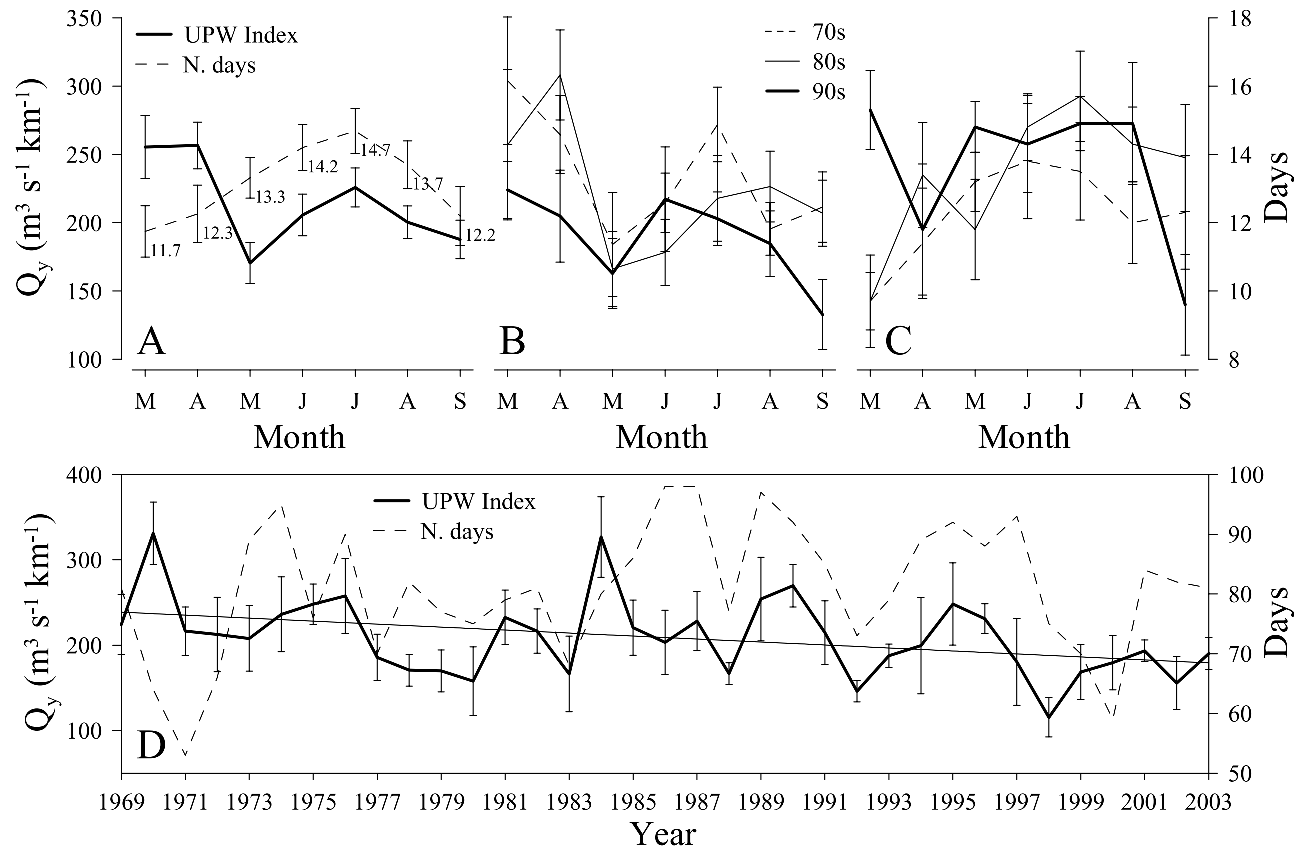

Figure 10. (a) Mean value and S.E. of positive Ekman transport (upwelling intensity) and number of days of positive values (upwelling frequency) per month (the latter is referred to the right-hand axis, mean values are typed), from March–September (1969–2003). (b) Intensity of upwelling per decades: 1970s, 1980s, and 1990s. (c) Number of days with upwelling per decades: 1970s, 1980s, and 1990s. (d) Intensity (Mean and S.E.) and number of days of upwelling per year averaged from April–September values. The straight line is the linear fit for intensity.

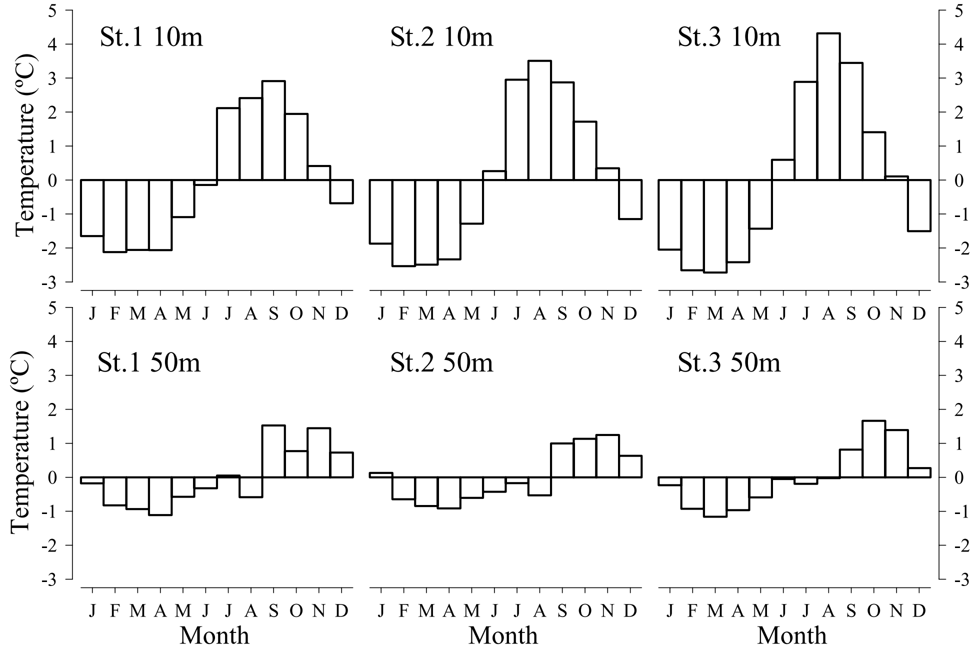

Figure 11. Temperature seasonal cycles. Monthly seasonal indices of temperature series at 10 and 50 m at the three stations. The fractions of variance and trends are shown in Table 1. Negative and positive deviations are referred to the mean level of the series in °C.

The most saline months corresponded to November–February coinciding with the period when the IPC reaches the region. Temperature at these depths showed a similar seasonal cycle (Figure 12). Salinity decreased through the whole water column at the most oceanic station (Table 2) being more pronounced in the uppermost 50 m (from -0.013 yr^{-1} to -0.017 yr^{-1}). Similar trends were detected below 10 m at the middle station and below 20 m at the coastal one.

3.6. Time Series of Density

[35] Divergences in the long-term evolution of density at different depths can be used to infer changes in the strength of the water column stratification. Negative trends were detected as deep as 30 m at the outermost station and at the surface at St. 2 (Table 3) resembling the coastal-oceanic gradient detected in temperature.

4. Discussion

[36] The temporal and spatial scales covered by this database grant an integrated view of the hydrographic variability in the region. Our results illustrate these processes, ranging from the interannual changes of Central Waters to the long-term trends of individual time series.

[37] The geostrophic circulation in the Bay of Biscay is known to be weak and slow [*Pingree*, 1993; *Bower et al.*, 2002]. This lack of a dominant circulation pattern makes water masses depend much more on the regional climatic conditions, i.e., rainfall, river flows, storms, etc. Local meteorology did not support a direct effect of the regional climate on Central Waters but there was a lagged effect of the North Atlantic Oscillation.

[38] Off Galicia, *Pérez et al.* [2000] reported a positive correlation between the NAO index and the year-to-year variations of salinity on the 27.1 isopycnal. The authors explained it in relation to wind direction and precipitation on the intergyre region. Our results differ from this in that the correlation is negative what agrees with the lack of relation with local meteorology.

[39] The NAO is the dominant mode of winter climate variability in the North Atlantic region. During its positive phase, increased wind speed transports heat and moisture

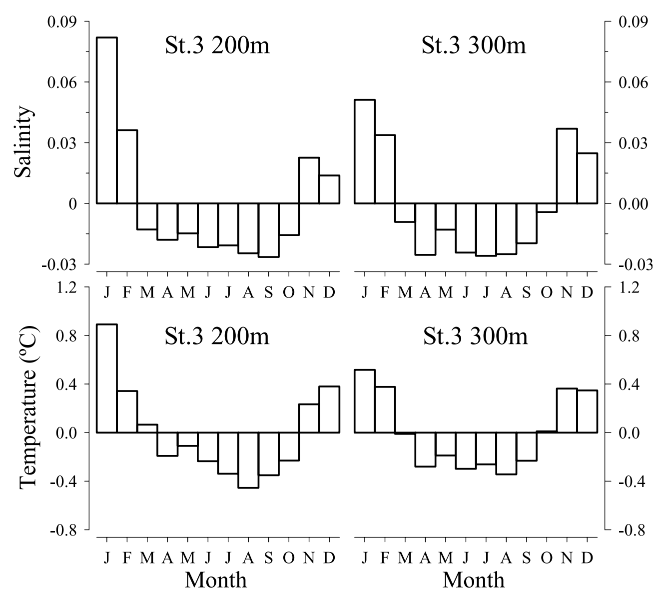

Figure 12. Salinity seasonal cycles. Monthly seasonal indices of salinity and temperature series at Station 3 (200 and 300 m). The fractions of variance and trends are shown in Table 1. Negative and positive deviations are referred to the mean level of the series.

over northern Europe, also increasing the number and intensity of storms (see review in work by *Hurrell et al.* [2003]). These conditions are likely to strongly modify the typical ENACW signature and at the same time enhance the formation of Mode Waters on the Celtic-Armorican shelf.

[40] The variability of Central Waters in the bay has been approached almost exclusive in terms of isopycnal mixing in recent literature [*van Aken*, 2001; *Huthnance et al.*, 2002]. However, the winter climate anomalies at the subduction area of the ENACW seem not to fully explain the variation observed at these latitudes [*González-Pola et al.*, 2005].

[41] The signature of the BBCW can be also found further east, around Cap Ferret [*Valencia et al.*, 2004]. It is possible that this water body expands or contributes to the ENACW to a greater extent during some years. Further studies on a greater spatial scale will be required to adequately describe the mechanism through which Central Waters respond to the NAO forcing and the role of the BBCW. From our fixed approach we cannot properly conclude on advection but it may be more important than previously assumed.

[42] To our knowledge, this is the first time that the Iberian Poleward Current (IPC) is investigated through a time series of T-S diagrams. Our results show that the particular thermohaline background does not affect its arrival in the region. January records of SSTs have been commonly used to characterize its year-to-year intensity as it is supposed to be fully developed on that month [*García-Soto et al.*, 2002; *Álvarez-Salgado et al.*, 2003]. However, the IPC flow usually lasts for several months (November–February) and January does not always correspond to the maximum strength every winter. Our results showed that layers above its core are always more or less affected by desalinization and cooling. Therefore infrared satellite images (AVHRR) should not be considered a good proxy for measuring its intensity since other mechanisms than the IPC can lead to SST variations.

[43] The strong IPC years described in this work matched with those detected in the region by *García-Soto et al.* [2002] through AVHRR. However, in the winter of 2002–2003 a positive SST anomaly was related to a strong IPC incursion in the bay [*García-Soto*, 2004] which is not supported by our data. Moreover, this winter, together with 2001, proved to be the least saline winter of the series. As a possible explanation for this discrepancy we point at spatio-temporal asynchronies in the winter deep mixing between water masses on the continental shelf/slope and the deeper open seawaters. Thus the deeper mixing offshore could possibly lead to a stronger cooling of the whole water column unlike shallow waters (less prone to such an intense heat loss) causing this thermal structure.

[44] The IPC also showed great vertical variability. Interestingly, a marked double-core structure was seen in January 1996 and February 2002. This current is known to flow west-east in the south of the bay and so this structure may suggest two currents circulating one on top of the other. The mechanism behind it surpasses the objective of this work. However, intensive oceanographic sampling carried out on a wider spatial grid [*González-Quirós et al.*, 2004] has shown evidence of a meandering flow of the IPC in the region as well as eddy generation [*Pingree and Le Cann*, 1992a, 1992b; *Gil*, 2003]. The sampling strategy based on a single transect imposes a spatial limitation when trying to identify the factors responsible for this particular structure. It is possible, as pointed out above, that under extremely favorable conditions, two intrusions superimpose but it may also be a consequence of the described meandering pattern. Contrary to *García-Soto et al.* [2002], our results do not support a causal relation between the NAO index and the IPC. Winds seem also not to determine the IPC flow in our region although there may be a small modulation effect, as stated by *Frouin et al.* [1990].

[45] Despite this great diversity of hydrographic processes, upper layers are by and large driven by midlatitude seasonality and consequently the annual cycle accounted for the bulk of the variance of temperature series. Upwelling proved to be the most important mesoscale process on the coast being to a large extent responsible for the coastal-oceanic gradient of warming. The positive trends of temperature were associated with a greater importance of the seasonal cycle and therefore less influence of upwellings. Temperature has very conceivably increased in the whole area at approximately the same rate. However, the distorting effect of the upwelling, together with tides and wind mixing, counteracts this warming by increasing the relative weight of stochastic variance. This stochastic variability reaches its maximum at the most coastal station where the upwelling most strongly affect the typical cycle of warming and cooling observed in the open sea. On the other hand, the outermost station reproduces much better deep ocean dynamics where all these processes are of rather minor importance.

[46] The *Intergovernmental Panel on Climate Change* [1996] estimated an average warming of approximately 0.6°C at Earth's surface during the past 100 years. Under this global warming scenario, *Levitus et al.* [2000] reported a net warming in the Atlantic since mid-1950s, in particular after the mid-1970s when it entered a warm state. Regional analyses of temperature time series in the Bay of Biscay revealed increasing trends since the 1970s [*Valencia*, 1993; *Pingree*, 1994; *Soletchnik et al.*, 1998; *Lavín et al.*, 1998; *Cabanas et al.*, 2003; *Woehrling et al.*, 2005] although the different statistical techniques employed renders intercomparison of slopes difficult.

[47] *Koutsikopoulos et al.* [1998] defined the sea surface temperature (SST) long-term and periodic components for the Bay of Biscay using a grid of data based on vessels and buoys measurements from 1972 to 1993. By using the empirical model coefficients for the area concerned we have recreated the series from 1993–2003 in order to compare both trends. The model predicted an interestingly similar positive trend (0.050°C yr^{-1}) to that detected at the oceanic station (0.055°C yr^{-1}).

[48] Recently, *Planque et al.* [2003] showed a positive trend of 0.6°C per decade in SST (from Météo-France) in the inner part of southern Bay of Biscay where the warming is known to be slightly higher. The much longer time span provided by COADS records reveals the existence of oscillations in the evolution of SSTs from 1844 to 2000 [*Planque et al.*, 2003]. *Southward and Boalch* [1994] suggested the existence of natural oscillations superimposed on the anthropogenic warming. Therefore the trends reported here must be considered for the period of study and are prone to change in the future. Our results confirm that the previously detected warming in the area is developing at nearly the same rate since 1972 and report its penetration down to 20 m depth.

[49] A decreasing density trend was detected as deep as 30 m following the coastal-oceanic gradient in a similar fashion to temperature. As density also accounts for salinity, this decreasing trend is consequence of the combined effect of the warming and freshening, both of which enhance stratification. Consequently, this could be an indication of an increasing stratification either in intensity or duration. A growing stratification will probably cause an enhancement of the oligotrophic conditions in summer, leading to a reduction in the global primary production. Moreover, it may also affect the structure of whole plankton community favoring the microbial food web at the expense of the classical food web [*Legendre and Rassoulzadegan*, 1995]. Eventually, upper trophic levels will be affected by any change in the upward channeling of the marine production [*Beaugrand et al.*, 2003].

[50] Under such an increasing temperature and stratification scenario, any change in upwelling intensity or its seasonal window could have a key effect on the regional ecology. At present, together with the more important continental influence toward the inner part of the Bay, upwellings are responsible for an E-W temperature gradient along the Cantabrian coast [*Koutsikopoulos et al.*, 1998] which translates into an ecological gradient inshore communities [*Fischer-Piette*, 1957; *van den Hoek*, 1975; *Anadón and Niell*, 1981; *Alcock*, 2003]. From an overall perspective, upwelling/downwelling intensity has remained constant during the last 30 years. This upwelling system is characterized by many short-lived events concentrated around a favorable season rather than a nearly constant upwelling season. However, this structure is not at a standstill and seemed to have changed over decades resulting in overall advancement of the onset of the upwelling-favorable season.

[51] A change of this nature may have important implications. Thus an upwelling event occurring in March, when the water column is completely mixed, can be of minor importance to the biological system, while an upwelling in August, under strong stratification and nutrient depletion, should trigger off a phytoplankton bloom. In addition, a change in the upwelling seasonal window would also have an effect on the inshore retention (or dispersal) of some fish larvae (sardine, mackerel, anchovy, etc.) and other coastal organisms.

[52] *Bakun* [1990] postulated an intensification of the alongshore wind stress in the main upwelling systems of the world, including the western coast of the Iberian Peninsula, as consequence of global climate change. Specifically, he showed a positive trend in the 6-month (April–September) averages of monthly estimates of wind stress (1948–1979) off Galicia and Portugal. Such an increase might counteract the warming. However, decreasing trends of the upwelling season have more recently been reported off Galicia for the period 1970–2000 [*Lavín et al.*, 2000; *Cabanas et al.*, 2003]. Our results support the latter showing a decreasing trend in upwelling intensity since 1968. Hence upwelling intensity may have shifted from the previously increasing phase to a decreasing phase in the last 30 years.

[53] Supposing this decrease to continue, the spatial gradient detected in the amount of noise of temperature series might get reduced. This will most likely lead to a temperature increase in the upper layers and the intensification of the oligotrophic conditions in summer. In particular, the seasonal structure at middle station will approach that displayed at the most oceanic station (St. 3) with the subsequent ecological implications. Both a decreasing upwelling intensity or a change in its seasonal structure would also modify the distribution of some seaweeds as it has been documented [*Arrontes*, 1993] and predicted from GCM by *Alcock* [2003].

[54] **Acknowledgments.** This work was supported by a grant from the Ministerio de Ciencia y Tecnología [FPI fellowship] and continued with a grant from the University of Oviedo [FTDOC-04]. The Asturian time series sampling program was funded by the project "Control a largo plazo de las condiciones químico-biológicas de la Plataforma Continental de Asturias" (SV-02-IEO y SV-97-IEO-1) (U. de Oviedo/Instituto Español de Oceanografía) and "Excelencia Investigadora del Principado de Asturias 'Ecología de Ecosistemas Acuáticos'" (PR-01-GE-3) (FICYT, Principáu d'Asturies). We would like to thank the many people whose efforts helped to establish and keep up the time series database presented here, especially those from the Oceanography Group of the Areas of Ecology and Zoology of the University of Oviedo as well as the whole crew of oceanographic vessel *José Rioja*. Luis Valdés, coordinator of the IEO time series program, is especially thanked for his continuous support to the Asturian section. It is thanks to all of them that this work has been possible. Espen Bagøien and Julio Arrontes are thanked for providing valuable comments on the manuscript as well as the three anonymous reviewers whose suggestions greatly improved the original scope of this publication. Continuous temperature data (shown in Figure 8) were kindly supplied by the Intertidal Ecology Group of the University of Oviedo while CTD data off Galicia (shown in Figure 4) come from the project "Organización trófica y flujo de materiales en giros anticiclónicos (SWODDIES) en el Golfo de Vizcaya (GIGOVI)" (MAR96-1872-CO3-03) (CICYT, Ministerio de Educación y Ciencia). The Instituto Nacional de Meteorología, Puertos del Estado and Confederación Hidrográfica del Norte are also thanked for providing meteorological data.

References

Alcock, R. (2003), The effects of climate change on rocky shore communities in the Bay of Biscay, 1895–2050, Ph.D. thesis, Univ. of Southampton, Southampton, U. K.

Álvarez-Salgado, X. A., et al. (2003), The Portugal coastal counter current off NW Spain: New insights on its biogeochemical variability, *Prog. Oceanogr.*, *56*, 281–321.

Ambar, I., and A. F. G. Fiúza (1994), Some features of the Portugal current system: A poleward slope undercurrent, an upwelling related summer southward flow and an autumn-winter poleward coastal surface current, in *Proceedings of the Second International Conference on Air-Sea Interaction and on Meteorology and Oceanography of the Coastal Zone*, edited by K. B. Katsaros, A. F. G. Fiúza, and I. Ambar, pp. 286–287, Am. Meteorol. Soc., Boston, Mass.

Anadón, R., and F. X. Niell (1981), Distribución de macrofitos en la costa asturiana (N de España), *Invest. Pesq.*, *45*, 143–156.

Arrontes, J. (1993), Nature of the distributional boundary of *Fucus serratus* on the north shore of Spain, *Mar. Ecol. Prog. Ser.*, *93*, 183–193.

Bakun, A. (1973), Coastal upwelling indices, west coast of North America, 1946–71, *NOAA Tech. Rep. NMFS, NMFS-671*.

Bakun, A. (1990), Global climate change and intensification of ocean coastal upwelling, *Science*, *247*, 198–201.

Beaugrand, G., K. M. Brander, J. A. Lindley, S. Souissi, and P. C. Reid (2003), Plankton control of cod abundance in the North Sea, *Nature*, *426*, 661–664.

Blanton, J. O., L. P. Atkinson, F. Fernández del Castillejo, and A. Lavín Montero (1984), Coastal upwelling off the Rias Bajas, Galicia, northwest Spain I: Hydrographic studies, *Rapp. P. V. Reun. Cons. Int. Explor. Mer*, *183*, 79–90.

Bode, A., M. Varela, B. Casas, and N. González (2002), Intrusions of eastern North Atlantic central waters and phytoplankton in the north and northwestern Iberian shelf during spring, *J. Mar. Syst.*, *36*, 197–218.

Botas, J. A., A. Bode, E. Fernández, and R. Anadón (1988), Descripción de una intrusión de agua de elevada salinidad en el Cantábrico central: Distribución de los nutrientes inorgánicos y su relación con el fitoplancton, *Invest. Pesq.*, *52*, 561–574.

Botas, J. A., E. Fernández, A. Bode, and R. Anadón (1989), Water masses off the central Cantabrian coast, *Sci. Mar.*, *53*(4), 755–761.

Botas, J. A., E. Fernández, A. Bode, and R. Anadón (1990), A persistent upwelling off the central Cantabrian coast (Bay of Biscay), *Estuarine Coastal Shelf Sci.*, *30*, 185–199.

Bower, A. S., B. Le Cann, T. Rossby, W. Zenk, J. Gould, K. Speer, P. L. Richardson, M. D. Prater, and H.-M. Zhang (2002), Directly measured mid-depth circulation in the northeastern North Atlantic Ocean, *Nature*, *419*, 603–607.

Cabanas, J. M., A. Lavín, M. J. García, C. González-Pola, and E. Tel Pérez (2003), Oceanographic variability in the northern shelf of the Iberian Peninsula, 1990–1999, *ICES Mar. Sci. Symp.*, *219*, 71–79.

Chatfield, C. (1992), *The Analysis of Time Series, An Introduction*, 131 pp., CRC Press, Boca Raton, Fla.

Cooper, L. N. H. (1949), Cascading over the continental slope of water from the Celtic Sea, *J. Mar. Biol. Assoc. U. K.*, *28*, 719–750.

Draper, N., and H. Smith (1981), *Applied Regression Analysis*, 709 pp., John Wiley, Hoboken, N. J.

Falkowski, P. G., R. T. Barber, and V. Smetacek (1998), Biogeochemical controls and feedbacks on ocean primary production, *Science*, *281*, 200–206.

Fernández, E., A. Bode, A. Botas, and R. Anadón (1991), Microzooplankton assemblages associated with saline fronts during a spring bloom in the central Cantabrian Sea: Differences in trophic structure between water bodies, *J. Plankton Res.*, *13*, 1239–1256.

Fernández, E., J. Cabal, J. L. Acuña, A. Bode, A. Botas, and C. García-Soto (1993), Plankton distribution across a slope current-induced front in the southern Bay of Biscay, *J. Plankton Res.*, *15*, 619–641.

Fischer-Piette, E. (1957), Sur des déplacements de frontières biogéographiques, observés au long des côtes ibériques dans le domaine intercotidal, *Publ. Inst. Biol. Appl.*, *26*, 35–40.

Fraga, F., C. Mouriño, and M. Manríquez (1982), Las masas de agua de las costas de Galicia: Junio–Octubre, *Res. Exp. Cient.*, *10*, 51–77.

Frouin, R., A. F. G. Fiúza, I. Ambar, and T. J. Boyd (1990), Observations of a poleward surface current off the coasts of Portugal and Spain during winter, *J. Geophys. Res.*, *95*(C1), 679–691.

García-Soto, C. (2004), ‘‘Prestige’’ oil spill and Navidad flow, *J. Mar. Biol. Assoc. U. K.*, *84*, 297–300.

García-Soto, C., R. D. Pingree, and L. Valdés (2002), Navidad development in the southern Bay of Biscay: Climate change and swoddy structure from remote sensing and in situ measurements, *J. Geophys. Res.*, *107*(C8), 3118, doi:10.1029/2001JC001012.

Gil, J. (2003), Changes in the pattern of water masses resulting from a poleward slope current in the Cantabrian Sea (Bay of Biscay), *Estuarine Coastal Shelf Sci.*, *57*, 1139–1149.

Gil, J., L. Valdés, M. Moral, R. Sánchez, and C. García-Soto (2002), Mesoscale variability in a high-resolution grid in the Cantabrian Sea (southern Bay of Biscay), May 1995, *Deep Sea Res., Part I*, *49*, 1591–1607.

González-Pola, C., A. Lavín, and M. Vargas-Yáñez (2005), Intense warming and salinity modification of intermediate water masses in the southeastern corner of the Bay of Biscay for the period 1992–2003, *J. Geophys. Res.*, *110*, C05020, doi:10.1029/2004JC002367.

González-Quirós, R., A. Pascual, D. Gomis, and R. Anadón (2004), Influence of mesoscale physical forcing on trophic pathways and fish larvae retention in the central Cantabrian Sea, *Fish. Oceanogr.*, *13*(6), 351–364.

Haynes, R., and E. Barton (1990), A poleward flow along the Atlantic coast of the Iberian peninsula, *J. Geophys. Res.*, *95*(C7), 11,425–11,441.

Hidy, G. M. (1972), A view of recent air-sea interaction research, *Bull. Am. Meteorol. Soc.*, *53*, 1083–1102.

Holligan, P., and W. A. Reiners (1992), Predicting the responses of the coastal zone to global climate change, *Adv. Ecol. Res.*, *12*, 211–255.

Hurrell, J. W. (1995), Decadal trends in the North Atlantic Oscillation regional temperatures and precipitation, *Science*, *269*, 676–679.

Hurrell, J. W., Y. Kushnir, G. Ottersen, and M. Visbeck (2003), An overview of the North Atlantic Oscillation, in *The North Atlantic Oscillation: Climate Significance and Environmental Impact*, *Geophys. Monogr. Ser.*, vol. 134, edited by J. W. Hurrell et al., pp. 1–36, AGU, Washington, D. C.

Huskin, I., M. J. Elices, and R. Anadón (2003), Salp distribution and grazing in a saline intrusion off NW Spain, *J. Mar. Syst.*, *42*, 1–11.

Huthnance, J. M., H. M. van Aken, M. White, E. D. Barton, B. Le Cann, E. F. Coelho, E. Fanjul, P. Miller, and J. Vitorino (2002), Ocean margin exchange—Water flux estimates, *J. Mar. Syst.*, *32*, 107–137.

Intergovernmental Panel on Climate Change (1996), *Climate Change 1995: The Science of Climate Change, Contribution of Working Group I to the Second Assessment of the Intergovernmental Panel on Climate Change*, edited by J. T. Houghton et al., Cambridge Univ. Press, New York.

Isla, J. A., and R. Anadón (2004), Mesozooplankton size-fractionated metabolism and feeding off NW Spain during autumn: Effects of a poleward current, *ICES J. Mar. Sci.*, *61*, 526–534.

Karl, D. M., and A. F. Michaels (Eds.) (1996), Ocean Time Series: Results from the Hawaii and Bermuda Research Programs, *Deep Sea Res., Part II*, *43*.

Kiørboe, T. (1993), Turbulence, phytoplankton cell size, and the structure of pelagic food webs, *Adv. Mar. Biol.*, *29*, 1–72.

Koutsikopoulos, C., P. Beillois, C. Leroy, and F. Taillefer (1998), Temporal trends and spatial structures of the sea surface temperature in the Bay of Biscay, *Oceanol. Acta*, *214*(2), 335–343.

Lavín, A., G. Díaz del Río, J. M. Cabanas, and G. Casas (1991), Afloramiento en el noroeste de la Península Ibérica: Índices de Afloramiento para el punto 43°N 11°W. Período 1966–1989, *Inf. Tec. Inst. Esp. Oceanogr.*, *91*, 1–40.

Lavín, A., L. Valdes, J. Gil, and M. Moral (1998), Seasonal and interannual variability in properties of surface water off Santander, Bay of Biscay, 1991–1995, *Oceanol. Acta*, *21*(2), 179–190.

Lavín, A., G. Díaz del Río, G. Casas, and J. M. Cabanas (2000), Afloramiento en el noroeste de Península Ibérica: Índices de afloramiento para el punto 43°N, 11°O periodo 1990–1999, *Datos Resúm. Inst. Esp. Oceanogr 15.*, Inst. Esp. de Oceanogr., 25 pp., Madrid.

Legendre, P., and L. Legendre (1998), Ecological data series, in *Numerical Ecology*, *Dev. Environ. Modell.*, vol. 20, 2nd Engl. ed., pp. 637–705, Elsevier, New York.

Legendre, L., and F. Rassoulzadegan (1995), Plankton and nutrient dynamics in marine waters, *Ophelia Suppl.*, *41*, 153–172.

Levitus, S., J. I. Antonov, T. P. Boyer, and C. Stephens (2000), Warming of the world ocean, *Science*, *287*, 2225–2228.

Makridakis, S., and S. C. Wheelwright (1989), *Forecasting Methods for Management*, 5th ed., 480 pp., John Wiley, Hoboken, N. J.

Makridakis, S., S. C. Wheelwright, and V. E. McGee (1983), *Forecasting: Methods and Applications*, 2nd ed., 466 pp., John Wiley, Hoboken, N. J.

Mann, K. H., and J. R. N. Lazier (Eds.) (1991), *Dynamics of Marine Ecosystems: Biological-Physical Interactions in the Oceans*, Blackwell Sci., Malden, Mass.

Molina, R. (1972), Contribución al estudio del upwelling frente a la costa noroccidental de la Península Ibérica, *Bol. Inst. Esp. Oceanogr.*, *152*, 3–39.

Montgomery, D. C., L. A. Johnson, and J. S. Gardiner (1990), *Forecasting and Time Series Analysis*, 2nd ed., 381 pp., McGraw-Hill, New York.

Pérez, F. F., A. F. Ríos, B. A. King, and R. T. Pollard (1995), Decadal changes of the T-S relationship of the eastern North Atlantic central water, *Deep Sea Res., Part I*, *42*, 1849–1864.

Pérez, F. F., R. T. Pollard, J. F. Read, V. Valencia, J. M. Cabanas, and A. F. Ríos (2000), Climatological coupling of the thermohaline decadal changes in central water of the eastern North Atlantic, *Sci. Mar.*, *64*(3), 347–353.

Pérez, F. F., C. G. Castro, X. A. Álvarez-Salgado, and A. F. Ríos (2001), Coupling between the Iberian basin-scale circulation and the Portugal boundary current system: A chemical study, *Deep Sea Res., Part I*, *48*, 1519–1533.

Pingree, R. D. (1993), Flow of surface waters to the west of the British Isles and in the Bay of Biscay, *Deep Sea Res., Part II*, *40*, 369–388.

Pingree, R. D. (1994), Winter warming in the southern Bay of Biscay and Lagrangian eddy kinematics from a deep-drogued Argos Buoy, *J. Mar. Biol. Assoc. U. K.*, *74*, 107–128.

Pingree, R. D., and B. Le Cann (1990), Structure, strength and seasonality of the slope currents in the Bay of Biscay region, *J. Mar. Biol. Assoc. U. K.*, *70*, 857–885.

Pingree, R. D., and B. Le Cann (1992a), Anticyclonic eddy X91 in the southern Bay of Biscay, May 1991 to February 1992, *J. Geophys. Res.*, *97*(C9), 14,353–14,367.

Pingree, R. D., and B. Le Cann (1992b), Three anticyclonic slope waters oceanic eddies (SWODDIES) in the southern Bay of Biscay in 1990, *Deep Sea Res., Part A*, *39*, 1147–1175.

Planque, B., P. Beillois, A.-M. Jégou, P. Lazure, P. Petitgas, and I. Puillat (2003), Large-scale hydroclimatic variability in the Bay of Biscay: The 1990s in the context of interdecadal changes, *ICES Mar. Sci. Symp.*, *219*, 61–70.

Pollard, R. T., M. J. Griffiths, S. A. Cunningham, J. F. Read, F. F. Pérez, and A. F. Ríos (1996), Vivaldi 1991—A study of the formation, circulation and ventilation of Eastern North Atlantic Central Water, *Prog. Oceanogr.*, *37*, 167–192.

Ríos, A. F., F. F. Pérez, and F. Fraga (1992), Water masses in the upper and middle North Atlantic Ocean east of Azores, *Deep Sea Res., Part I*, *39*, 645–658.

Sherman, K., and H. R. Skjoldal (Eds.) (2002), *Large Marine Ecosystems of the North Atlantic: Changing States and Sustainability*, 464 pp., Elsevier, New York.

Siegel, D. A., , D. M. Karl, and A. F. Michaels (Eds.) (2001), HOT and BATS: Interpretations of open ocean biogeochemical processes, *Deep Sea Res., Part II*, *48*.

Soletchnik, P., N. Faury, D. Razet, and P. Goulletquer (1998), Hydrobiology of the Marennes-Oleron Bay. Seasonal indices and analysis of trends from 1978 to 1995, *Hydrobiologia*, *386*, 131–146.

Southward, A. J., and G. T. Boalch (1994), The effects of changing climate on marine life: Past events and future predictions, in *Man and the Maritime*

Environment, *Exeter Mar. Stud.*, vol. 9, pp. 101–143, Univ. of Exeter Press, Exeter, U. K.
Stenseth, N. C., G. Ottersen, J. Hurrell, A. Mysterud, M. Lima, K.-S. Chan, N. G. Yoccoz, and B. Adlandsvik (2003), Studying climate effects on ecology through the use of climate indices: The North Atlantic Oscillation and beyond, *Proc. R. Soc. London, Ser. B*, *270*, 2087–2096.
Tréguer, P., P. Le Corre, and J. R. Grall (1979), The seasonal variations of nutrients in the upper waters of the Bay of Biscay region and their relation to phytoplankton growth, *Deep Sea Res., Part A*, *26*, 1121–1152.
U. N. Educational, Scientific, and Cultural Organization (1984), La escala de salinidades prácticas de 1978 y la ecuación internacional del estado del agua de mar de 1980, *Doc. Téc. UNESCO Cienc. Mar 36*, New York.
Valencia, V. (1993), Estudio de la variación temporal de la hidrología y el plancton en la zona nerítica frente a San Sebastián entre 1988–1990, *Inf. Tec. Gobierno Vasco 52*, 105 pp., Gobierno Vasco, Vitoria-Gasteiz, Spain.
Valencia, V., J. Franco, A. Borja, and A. Fontán (2004), Hydrography of the southeastern Bay of Biscay, in *Oceanography and Marine Environment of the Basque Country*, *Elsevier Oceanogr. Ser.*, vol. 70, edited by A. Borja and M. Collins, pp. 159–194, Elsevier, New York.
van Aken, H. M. (2000), The hydrography of the mid-latitude northeast Atlantic Ocean II: The intermediate water masses, *Deep Sea Res., Part I*, *47*, 789–824.
van Aken, H. M. (2001), The hydrography of the mid-latitude northeast Atlantic Ocean—Part III: The subducted thermocline water mass, *Deep Sea Res., Part I*, *48*, 237–267.
van den Hoek, C. (1975), Phytogeographic provinces along the coast of the northern Atlantic Ocean, *Phycologia*, *14*, 317–330.
Woehrling, D., A. Lefebvre, G. Le Fèvre-Lehoërff, and R. Delesmont (2005), Seasonal and longer term trends in sea temperature along the French north coast, 1975 to 2002, *J. Mar. Biol. Assoc. U. K.*, *85*, 39–48.
Wooster, W. S., A. Bakun, and D. R. McLain (1976), The seasonal upwelling cycle along the eastern boundary of the North Atlantic, *J. Mar. Res.*, *34*(2), 131–141.

R. Anadón, M. Quevedo, and L. Viesca, Área de Ecología, Departamento de Biología de Organismos y Sistemas, Universidad de Oviedo, Catedrático Valentín Andrés Álvarez, E-33071 Uviéu/Oviedo, Spain. (ranadon@uniovi.es; quevedomario@uniovi; viescaleticia@uniovi.es)

R. González-Quirós, Centro de Investigación y Formación Acuícola y Pesquera (CIFAP) El Toruño, carretera N-IV Km. 654, Camino Tiro del Pichón, E-11500 El Puerto de Santa María, Cádiz, Spain. (rafael.gonzalezquiros.ext@juntadeandalucia.es)

M. Llope and N. C. Stenseth, Centre for Ecological and Evolutionary Synthesis (CEES), Department of Biology, University of Oslo, P.O. Box 1050 Blindern, N-0316 Oslo, Norway. (marcos.llope@bio.uio.no; n.c.stenseth@bio.uio.no)